Pulmonary Distribution and Kinetics of Inhaled [^{11}C]Triamcinolone Acetonide

Marc S. Berridge, Zhenghong Lee, and Donald L. Heald

Division of Radiology, Case Western Reserve University/University Hospitals of Cleveland, Cleveland, Ohio; and Medical Affairs, Rhône Poulenc Rorer Pharmaceuticals Inc., Collegeville, Pennsylvania

Triamcinolone acetonide (TAA) is an anti-inflammatory steroid used for topical treatment of allergic rhinitis and asthma. Drug deposition onto target tissues is an important parameter, so methods for accurate deposition measurement are needed. Lung deposition is especially problematic to measure because of the large field of view and low relative drug penetration. Our main objective was to use PET to measure the deposition and postdeposition kinetics of TAA in the lung after administration from the Azmacort inhaler. The second objective was to evaluate changes in distribution caused by the inhalation spacer that is built into the product. **Methods:** ^{11}C-labeled TAA was formulated as the Azmacort product, 5 healthy volunteers inhaled it, and PET scans were obtained of its distribution in the head and chest. Region-of-interest analysis with CT overlay was used to analyze the distribution and kinetics in the airway and lung. **Results:** From 10% to 15% of the inhaled drug dose was deposited in target airway regions in a distally decreasing pattern. Deposition in the oral cavity was about 30% of the dose. Slow absorption or clearance of drug from target tissues was observed over time. Use of the inhalation spacer caused statistically significant increases in all target tissues (factor of 2–5) and a roughly 40% decrease in oral deposition. Measurable amounts of the drug remained in target regions throughout the scanning period. **Conclusion:** Local pulmonary distribution and kinetics of inhaled drugs can be measured accurately by PET for drug development. The integrated actuator–spacer significantly enhanced deposition of TAA in target tissues and reduced deposition in the oropharyngeal region.

Key Words: PET; inhaler; pulmonary; biodistribution; triamcinolone acetonide; steroid; drug development; Azmacort

J Nucl Med 2000; 41:1603–1611

The pulmonary distribution of inhaled drugs for treatment of asthma is an important consideration in the design and use of the drugs. Inhalation delivery systems are designed to deposit corticosteroid at the desired sites of action to maximize therapeutic effects while reducing systemic steroid activity. Although a common practice to observe pulmonary drug distribution is to add ^{99m}Tc-labeled compounds to a drug preparation and perform planar γ imaging, that method is subject to quantitative and qualitative errors caused by regional variations in attenuation and scatter parameters as well as the chemical and physical differences between the tracer and the drug (*1–7*). In such studies, adherence to the tracer principle is a constant concern. PET allows quantitative 3-dimensional imaging of drug distribution as a function of time and, when correlated with anatomic imaging, can provide the information needed to accurately evaluate the deposition and absorption characteristics of a drug formulation or delivery device.

Triamcinolone acetonide (TAA) is a potent anti-inflammatory synthetic glucocorticoid (*8–12*) that is topically administered in several forms. One of those forms is Azmacort (Rhône Poulenc Rorer Pharmaceuticals Inc. [RPR], Collegeville, PA), a product approved by the Food and Drug Administration for treatment of asthma. The product consists of a TAA formulation in a pressurized metered-dose aerosol canister, with an actuator containing a nozzle to release and aerosolize the drug, which is integrated with a tubular spacer. In use, a patient inhales from the opposite end of the spacer while actuating the unit to release the aerosol dose. The spacer concept, which is supported by experimental evidence (*13–18*), is to increase pulmonary deposition of the drug by controlling the inhaled air stream and to decrease oral deposition of the drug by providing a surface for removal of large particles that do not effectively enter the inhaled air stream. Thus, the spacer is intended to limit systemic drug absorption while enhancing pulmonary deposition. The purpose of this study was to measure the regional pulmonary deposition of TAA from the inhaler and to evaluate the effect of the integrated spacer on distribution patterns. PET was chosen to provide regions of interest with 3-dimensional accuracy and to reliably and quantitatively measure deposition of the drug in each region. TAA was radiolabeled with ^{11}C and incorporated into the TAA formulation so that the imaging measurements could be relied on to represent the distribution and kinetics of the deposited active ingredient of the drug formulation. Healthy volunteers were studied because the experimental question was, first, to measure the amount of drug that is deposited in the lung and, second, to determine if the integrated spacer has any detectable effect on that distribution. The presence of asthma of various degrees of severity would be expected to change the amount and the individual variability of drug deposition but not to alter any trend observed for spacer effect in healthy individuals. For this study, we believed that

Received Sep. 28, 1999; revision accepted Feb. 1, 2000.
For correspondence or reprints contact: Marc S. Berridge, PhD, Division of Radiology, University Hospitals of Cleveland, 11100 Euclid Ave., Cleveland, OH 44106.

the important goals were to establish a quantitative baseline and to avoid the possibility that individual variations in disease would obscure the measured effect of the spacer.

MATERIALS AND METHODS

Subjects

Five healthy male volunteers (age range, 20–45 y; weight range, 59–88 kg) were recruited for the study. For this initial study, male volunteers were chosen for consistency in the small sample and in consideration of privacy and modesty for presentation of the 3-dimensional rendered anatomic data. All volunteers were experienced in the use of oral inhalers. Some had a history of mild asthma, which currently did not require regular treatment; others had used an inhaler for other reasons. The enrolled volunteers gave informed consent for the study, which was approved by the University Hospitals of Cleveland Institutional Review Board and Radiation Safety Committee. Inclusion criteria were an age between 18 and 50 y and normal airway anatomy and function (forced expiratory volume in 1 s [FEV_1] $\geq$ 80% of that predicted). Exclusion criteria were a body weight more than 15% greater than or less than the ideal body weight as specified by standard tables (Metropolitan Life Insurance Company, New York, NY); a history of chronic disease of the upper or lower airway; any smoking within the past 2 y or a smoking history of more than 10 (pack/day)-years; a history of significant cardiovascular, neurologic, hepatic, renal, or respiratory conditions; a history of any other condition deemed by an examining physician to potentially interfere with the study; clinically relevant deviations from normal findings or evidence of drug abuse on general physical examination or laboratory testing (basic blood chemistry analysis, complete blood count with differential urinalysis, spirometry FEV_1); or hypersensitivity to corticosteroids. Postadmission exclusion criteria were the development of an illness or use of medications that could affect the mucosa, airways, or respiratory function.

Study Protocol

Prospective volunteers, after giving informed consent, underwent screening consisting of the physical examination and laboratory tests. Accepted volunteers were trained in the use of the inhaler, tested for correct external technique, and warned to keep the airway open by avoiding raising the tongue during inhalation. Training involved at least 2 practice sessions before the first scan and a refresher session before each scan. Two PET scans and a CT scan were obtained for each volunteer. At least 3 d passed between the 2 PET sessions to allow any potential effects of the drug to subside. Nine radiopaque fiducial markers were used to assist image registration. Three were within the field of view of each of the 3 bed positions. Permanent ink was used between scan sessions to record the positions of the markers. The initial ^{11}C-labeled PET scan was obtained with a random factor determining whether the spacer would be used. The second PET scan was obtained so that each volunteer had a study that used the integrated actuator–spacer and a second study that used the actuator from which the spacer had been cut off. Two volunteers used the spacer for their first scan, and 3 used the actuator without spacer for their first scan. After the first PET scan, the CT scan was obtained, and the volunteer returned at least 3 d later to complete the second PET scan.

PET

The scans were obtained using a 47-slice Exact scanner (Siemens/CTI PET Systems Inc., Knoxville, TN) in 2-dimensional mode. The volunteers were initially positioned supine in the scanner, lightly restrained with a chest strap to help maintain positioning and support the arms, and marked for repositioning using a laser system. The inhaled drug distributes over an area of interest that extends from the mouth through the entire lung. Because the PET scanner has a 15-cm-deep field of view, we needed to use 3 positions of the scan bed, and 3 separate scans, to include the entire volume. An initial attenuation scan was obtained in each of the 3 bed positions. During this scan, the fiducial markers were filled with a metal plug to facilitate their detection on the attenuation scans. The metal was removed at the end of the PET emission scan to avoid altering the local attenuation factors during the emission measurements and to allow CT scans to be obtained without creation of severe reconstruction artifacts. After the attenuation scan and before the emission scan, the center of each marker was loaded with 10 μL (20–100 kBq [0.5–3 μCi]) ^{11}C-labeled solution for detection of the markers on the emission scan. The inhaler canister was then assayed and weighed, assembled with an actuator (with or without the spacer, as needed for the scan), and given to the volunteer for self-administration. The volunteer took 4 inhalations at timed 30-s intervals, as described in the package insert. After each inhalation, the volunteer exhaled through a charcoal filter to collect any TAA that remained in the air stream. After the administration, the volunteer was instructed to avoid swallowing during repositioning in the scanner and during the initial attenuation scan series. The volunteer was then instructed to swallow before the beginning of the emission series and ad lib thereafter. The canister was weighed, and its radioactivity content was assayed again after the administration. Residual drug on the actuator, or actuator–spacer, was measured, and the particle size distribution in the canister was determined by cascade impactor assay. PET scans were acquired until 90 min after administration. The first bed position was the mouth, the second was the upper lung, and the third was the lower lung. The series was repeated at intervals. Three-scan series began at 0, 4.5, 9, 14, 30, 47, 64, 80, 112, and 145 min, so that a sequence of 10 images spanning the scan duration was acquired in each bed position. The initial 3 scans were acquired for 1 min in each bed position, the next 4 were acquired for 5 min each, and the last 2 were acquired for 10 min each. Approximately 1.5 min were required for bed motion during each group of 3 bed positions. Volunteers who felt unable to avoid swallowing until the designated time were asked to rinse their mouth with water instead and expectorate into a cup, which was then quantitatively assayed for collected drug.

Radiopharmaceutical

The ^{11}C radiolabeling and purification of TAA, the active ingredient of the formulation, have been reported (*19*). Briefly, the labeling process consisted of reaction of ^{11}C-labeled acetone with triamcinolone to produce the acetonide, which was then purified by HPLC. The labeled compound is stable, remaining unchanged for its useful lifetime. The commercial formulation was kindly provided for the study by RPR. The ^{11}C-labeled TAA (200–1600 MBq [5.5–45 mCi]; 0.7 mg) was dissolved in ethanol (40 μL) and added to the commercial preparation. The inhaler formulation contains a small amount of ethanol as a cosolvent, and the amount of ethanol and carrier TAA in the labeled preparation was controlled to ensure that they did not cause the composition in the canister to vary from manufacturing specifications. Additions were through a rubber septum (butadiene acrylonitrile), which was fitted to the canisters before filling. The septum fitting, the canister filling, and product

FIGURE 1. Intermediate step in lung region definition. Single-slice lung region boundary, as defined by semiautomatic region-growing method, is shown (A and B), with 3-dimensional region formed by combining regions defined on individual slices (C).

stability testing of the filled canisters were performed at RPR to ensure that the product met manufacturing standards. Canisters used in the study were returned to RPR after complete radioactive decay for additional assays to ensure that the product used during the study complied with specifications. After administration to the volunteer, a series of 10 actuations was performed from the same canister into a Delron cascade impactor using a new actuator with a spacer. Particle size was then determined. The TAA rinsed from the 2 actuators and the stages, elbow, filter, and casings of the cascade impactor was collected using quantitative techniques, and measured aliquots were assayed for radioactivity content. The fractions were also returned to RPR for TAA mass analysis. In this way, the dose delivered from the canister, the amount of drug deposited on the actuator, and the distribution of drug mass and radioactivity among particle sizes were verified to comply with the product specifications.

CT

Fast spiral CT with 0.75-s gantry rotation was performed using a Somatom 4+B scanner with power package (Siemens Medical Systems, Inc., Iselin, NJ). A bed speed of 8 mm/s with 3-mm collimation was used. The entire head and thorax were scanned to approximately the position of the diaphragm. During the scan, the fiducial markers were filled with a saturated calcium chloride solution. The acquisition began at the diaphragm and scanned toward the head while the volunteer held his breath. Each volunteer was instructed to ventilate and then to exhale to the point of a normal resting chest position, as opposed to the chest extension associated with a deep breath, before holding his breath. The volunteers were able to maintain the breath hold until the end of the scan, which lasted nearly 1 min. Scanning from the diaphragm minimized the effects of small involuntary chest movements during the last seconds of the procedure. Three-dimensional image data were reconstructed to an in-plane resolution of 0.976 mm/pixel, with a 4-mm interval between planes.

Image Analysis

A computer network for data reconstruction and manipulation was used with programs and algorithms developed for the purpose. PET data from the transmission scans were reconstructed into images of tissue density. The transmission PET images were then aligned with the CT images, which were the reference (fixed) volume. Regions of interest were created initially on image slices through the volume set (Fig. 1) to form 3-dimensional regions (Fig. 2). The rigid-body transformations (translation and rotation) were performed in 6 degrees of freedom. A graphical user interface (GUI) (Fig. 3, workspace area) was developed to enable registration with a precision of 2 mm in translation and 1 degree in rotation, using a combination of manual methods and the technique described by Woods et al. (*20*). The GUI simultaneously displays 3 views (axial, sagittal, and coronal) sliced from the volume of the PET and CT scans. In a third row, the pseudo–color overlay of the 2 is displayed. A set of slider controls allows a user to rotate and translate the PET transmission data along any of the 3 axes. Another set of sliders allows the user to move the display slices on each axis within the volumes, with synchronization of the 3 views and continuous updating of the display. PET emission images were reconstructed with camera calibration factors and attenuation correction, using the measured attenuation values from the transmission image, to express the data in units of radioactivity per milliliter of body volume. Decay corrections were made to the time of administration from the mid time of each scan, and the independently measured amount and specific activity of drug administered were used to convert the radioactivity units to units of deposited drug mass and percentage of administered dose. Each PET emission image set (from 47 data slices having an axial resolution of 3.375 mm and a transaxial resolution of 4.225 mm) in the

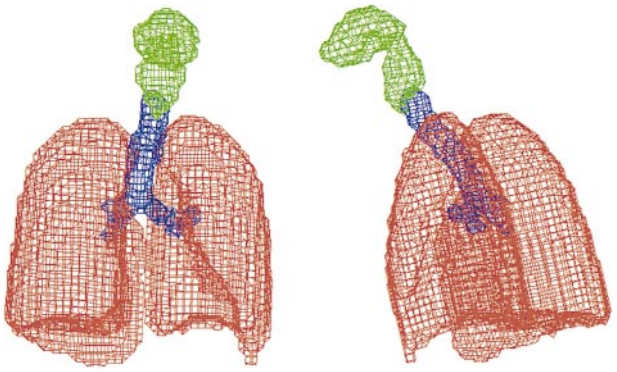

FIGURE 2. Example of 3-dimensional regions of interest created for 1 scan. Brown = whole lung; blue = trachea and main bronchi combined; green = nontarget region, mouth, and throat.

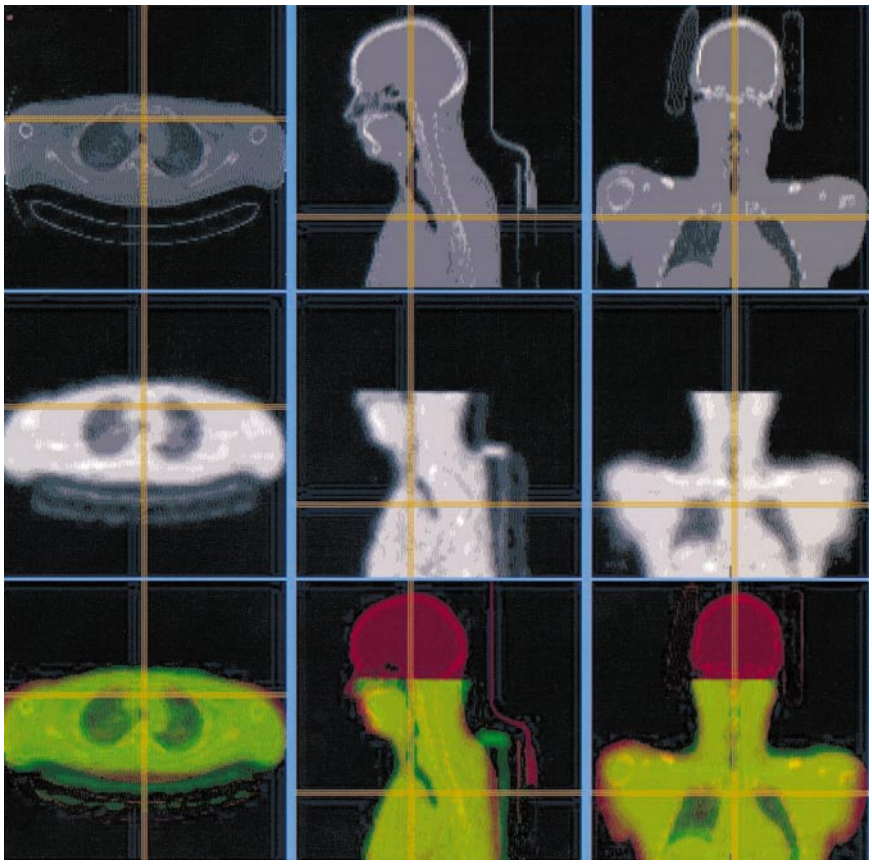

FIGURE 3. The GUI used for image registration. Shown are transaxial, sagittal, and coronal views (left to right) of selected slices from image volume sets of (top to bottom) CT, PET transmission, and pseudo–color overlay of the 2 (CT in red, PET in green). Yellow crosshairs show locations on each slice of 2 orthogonal slices. Slide bar controls (not shown) for each plane allow selection of slice displayed and control rotation and translation of PET data within its volume.

reconstructed dynamic series was interpolated to generate a 3-dimensional volume set of 4-mm^3 voxels for registration with the CT image. The alignment was performed, using the same GUI and a similar procedure, by first aligning the PET emission data with their transmission scan and then aligning the set of emission scans with the CT image, using the information in the transmission scan. With a rigid-body transformation for alignment, not all body parts can be aligned at the same time because of differences in body curvature, tidal breathing, and other motions. In all studies, the large airways and lungs were emphasized to ensure that these crucial regions were closely registered between PET and CT. As a consequence, the arms, shoulders, and hands were not aligned in some cases. Anatomic landmarks (bones, bronchial bifurcations, heart, body surface) and fiducial markers were used to position the scans. Regions of interest were defined using the CT scans and a combination of methods. Regional boundaries within each transaxial slice were verified visually and adjusted, if necessary, after creation of the regions. The overlay of CT and PET scans was then rendered in various 3-dimensional display modes (Fig. 4) to allow visual perception of the data.

The whole-lung regions were drawn to correspond to the outline of the lung from the CT images. A semiautomated technique (*21*) was used in which a ''seed'' was placed and allowed to ''grow'' to the edges of the lungs within the x–z plane of the volume set. The operation was repeated for each x–z plane (slice) in the set (Fig. 1). The region extended from the outer edge of the lung to the border of the bronchial region. At the hilus of the lung, manual editing was required to define the boundary of that part of the lung. The collection of these 2-dimensional regions on each x–z slice formed the 3-dimensional lung region shown in Figure 1 (right panel). The bronchial region was excluded, but more distal portions of the bronchial tree were included.

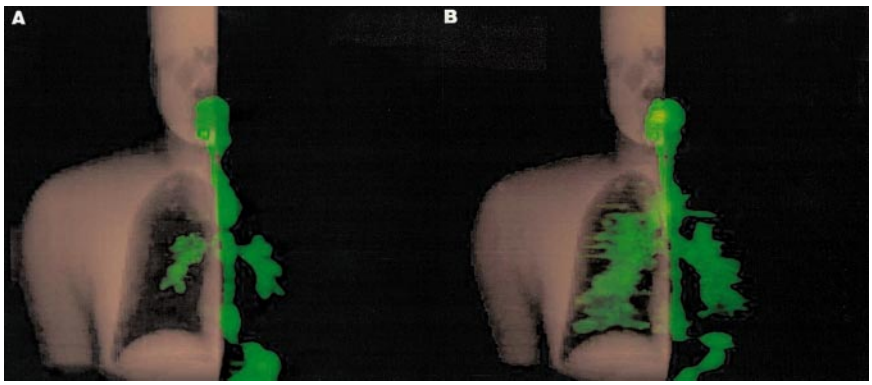

FIGURE 4. PET images of TAA deposition without (A) and with (B) use of spacer during inhalation.

The mid-lung region was placed as a perfect ellipsoid:

$$\frac{x^2}{a^2} + \frac{y^2}{b^2} + \frac{z^2}{c^2} = 1 \qquad \text{Eq. 1}$$

where a = 8.8 cm, b = 8.8 cm, and c = 21.0 cm. Because lung size varies between individuals, small adjustments were made to center the region within the lung. The region included approximately two thirds of the length and width of the lung, placed such that the entire bronchial tree to the third generation of bifurcations was included, with the surface as equidistant as possible from that level of bifurcation. For individual fitting, the 3 parameters were allowed to vary by ±2 cm. After placement of the ellipsoid, the bronchial region was excluded, leaving the mid-lung region. The mid-lung region is a subset of the whole-lung region.

Bronchial regions were drawn on the PET emission scans because they contained significant radioactivity and were clearly identifiable on the PET image. Use of the PET scan also ensured that any slight body movements would be considered to be within the region. The region-growing technique was again used to create irregular tubular regions. The seed was grown to a threshold of radioactivity chosen to place the distal border of the region at the second to third generation of bronchi. The proximal border was manually defined at the first bifurcation.

The trachea region was created on the CT scan, where it was clearly visible, again using a region-growing technique to match its outer edges. The trachea region extended from the edge of the mouth region to the edge of the bronchus regions and was verified against the PET scans.

The mouth region included essentially the entire head to approximately the level of the larynx, although drug was observed in the oral cavity, where the deposition was intense. Like the lung region, all of these regions are in 3 dimensions. Figure 2 shows 2 views of these regions along with the previously defined lung regions. The esophagus, like the bronchi, was small, position-sensitive, and difficult to detect on CT. Therefore, the esophagus region, too, was created on the PET emission scans. It could be seen on the emission scan separately from the trachea. A line was manually drawn through the visible trace of radioactivity in the esophagus and then was dilated to a circular cross-section to include the entire visible region. The region was then manually adjusted against the PET image to ensure that fiducial markers were excluded.

The abdomen region was created to quantify the radioactivity that was swallowed. With only 3 bed positions, the entire abdomen was not observed. The region therefore included all of the stomach and portions of the liver and intestine.

Summary regions were created by combining the basic regions. The outer-lung region was the sum of both whole-lung regions, minus the mid-lung region. The outer-lung region represented the most peripheral part of the lung. The mid-lung and bronchial tree regions were simply the sum of the respective left and right regions. The bronchial tree region represented the innermost lung, and the mid-lung region represented the most proximal portions of the lung beyond the bronchial region. The target-tissue region was defined as the sum of both whole-lung regions and both bronchi, including all potential target regions. The lung-plus-airway region was the sum of the target tissues and trachea, thereby including the entire air passage to the most distal part of the lung.

Regional data were obtained by mapping a region onto the sequence of emission volumes and adding up all the activities within the defined region for each volume. The results were expressed as time–dose curves in each region of interest. The deposition data were decay corrected to give the percentage of the independently measured administered radioactive dose of TAA in each region as a function of time. This value was expressed as the amount of drug deposited in each region, using the specific activity measurements made at the time of scanning. The radioactivity in each region was corrected for background counts by subtracting from each voxel the average value of voxels in several large background regions drawn outside the body on the same PET scan.

Much of the data of interest came from regions in the lung. Because the inhaled drug is deposited most strongly in the oral cavity, with decreasing deposition as the particles move distally, the regions of greatest interest received the least drug. The radiation dose to the oral cavity was the dose-limiting factor in the study and resulted in low counting rates in lung regions. To minimize statistical variations in the low-count regions, the individual time-point data were combined for analysis into 2 temporal regions, early (0–15 min) and late (15–90 min). The combined early and late data were used to analyze regional distribution and statistically compare the groups. Individual time-point data were used only to examine regional kinetics of the drug.

Accurate quantification in low-count regions, including background and scatter corrections and camera response at low counting rates, was verified by a series of phantom studies. A chest phantom was constructed consisting of tubes of radioactivity to represent the esophagus, trachea, and bronchi, with lung regions surrounding them. Each region was filled with a quantity of ^{11}C that was within the range of the quantities observed in the study. The regional measured radioactivity concentrations by PET were within 15% of the known concentration values. In addition, the dose of ^{11}C injected into each of the fiducial markers during each study was recorded. Additional regions of interest were defined around each marker (9 per scan), and the quantification of the marker doses was found to agree (within ±10%) with the nominal loaded dose. Although only 5 people participated in the randomized 2-way crossover study, statistical analysis was performed. The statistical significance as measured by *t* tests was similar to the statistical data shown, because of the large observed differences between groups. However, because of the small sample size, large variability in the data was expected and a simple *t* test was not appropriate. A typical and more meaningful treatment for this variability is to analyze the difference using log ratios. ANOVA was used to test for differences in the log response using SAS (PROC GLM) (SAS Institute, Cary, NC).

RESULTS

An Azmacort canister contains 20 g material, of which 60 mg is TAA and 200 mg is ethanol. The canisters modified for injection of tracer were loaded to meet the same specifications. Each canister was depleted by 150 actuations, which reduced the contents by about half. The radiolabeled TAA consisted of 0.7 mg TAA dissolved in 40 μL ethanol, and the manufacturing specifications for the product allowed the addition of up to 23 mg TAA and 80 μL ethanol. After use, the canisters were sent to RPR, where compliance with those specifications was verified. The Delron cascade impactor measured particle sizes from 0.5 to 16 μm. The results of the radioassays from the cascade impactor for each canister were analyzed at RPR using the procedures approved for the product. If any canister had failed to meet the product

specifications for particle size distribution of mass or of radioactivity, the affected volunteer would have been removed from the study. The volunteers received a mean ± SD of 528 ± 129 μg TAA and 8.5 ± 8.3 MBq (230 ± 225 μCi) ^{11}C label. Variations in radiation dose were caused by variations in yield of the synthesis and injection into the canister of labeled TAA, whereas variations in the inhaled mass were mainly caused by differences in inhalation efficiency with and without the spacer. Less than 1% of the inhaled dose was found as exhaled drug, and less than 1% of the dose was recovered from the mouth rinse in the 1 instance in which rinsing was performed.

Table 1 shows the distribution of TAA among the regions of interest. All individual regions and summary regions are shown, averaged for both periods treated. A systematic difference in deposition is seen between the left and right bronchi and lungs. This difference is consistent with the asymmetry of the lung anatomy. When the spacer was used, an average of 42% of the dispensed dose was deposited on the actuator and spacer, but only 12% of the dispensed dose was deposited on the actuator when no spacer was used. Therefore, the total mass of drug inhaled by the volunteers when the spacer was not used was 52% greater than when it was used. Although less drug was entering the mouth with the spacer, more drug was entering the lungs. If the amount of drug deposited in each region is expressed as a percentage of that which passes the actuator–spacer and enters the mouth, the average ratio of spacer to nonspacer deposition for any region rises by a factor of 1.5. Adjusting the amount of drug dispensed at the canister (by changing the number of puffs inhaled, or by changing the metered dose dispensed by the actuator) is easy. Delivery relative to the amount inhaled rather than to the amount dispensed is therefore more relevant in evaluating the performance of a delivery device relative to systemic absorption.

Table 2 shows the amount of TAA deposited in the major composite regions of interest as a percentage of inhaled dose. The difference and the ratio of deposition with spacer relative to deposition without spacer are also given, along with the ANOVA-derived probability value. The mouth (DDV) values represent oral deposition as it is commonly reported in the inhalation drug literature: the sum of the mouth, esophagus, stomach, and abdomen regions expressed as a percentage of the dose delivered at the valve (DDV) as opposed to the inhaled dose. The difference is the dose deposited on the spacer, which can be substantial. Mouth (DDV) is a more appropriate way to evaluate spacer performance but is less relevant to clinical use of the device. In every region but the mouth, the differences in deposition were statistically significant at the 0.05 level. Because the relative mouth deposition was reduced by the spacer, and because the spacer also directly reduced the total deposition, the statistical significance of the relative decrease was marginal ($P = 0.07$). However, when the mouth deposition

TABLE 1
Distribution of TAA Among Regions of Interest

Region	Spacer (μg)			No spacer (μg)			Difference (%)		
	Initial	Early	Late	Initial	Early	Late	Initial	Early	Late
Individual									
Left outer lung	8.9	8.3	3.7	5.9	5.3	2.9	51	55	28
Right outer lung	9.9	9.1	5.8	5.0	5.3	4.2	97	72	37
Left mid lung	6.1	4.8	1.5	2.7	2.7	0.9	128	79	58
Right mid lung	7.0	5.7	1.7	3.3	2.9	0.9	110	93	85
Left bronchial	12.2	10.2	2.5	2.3	2.7	0.7	427	282	245
Right bronchial	15.5	13.7	3.1	4.0	3.8	0.8	287	261	300
Trachea	17.1	12.5	3.4	9.9	9.6	2.9	72	31	18
Abdomen	68.2	109.0	156.0	35.2	130.0	174.0	94	−16	−10
Esophagus	26.8	27.5	20.2	45.6	42.0	20.3	−41	−35	−1
Mouth	157.3	157.0	100.0	266.6	258.0	171.0	−40	−39	−41
Groups									
Outer lung	18.8	17.3	9.4	10.9	10.6	7.1	72	63	33
Mid lung	13.1	10.5	3.2	6.0	5.6	1.9	118	86	72
Bronchial tree	27.8	23.9	5.6	6.3	6.5	1.5	338	270	273
Target tissues	59.6	51.7	18.3	23.2	22.7	10.5	157	128	75
Lung + airway	76.7	64.0	22.0	33.1	32.0	13.0	131	99	62
Abdomen + esophagus	95.0	137.0	176.0	80.8	172.0	194.0	17	−20	−9
Mouth	157.3	157.0	100.0	266.6	258.0	171.0	−40	−39	−41

"Initial," "Early," and "Late" represent first acquired data point, average of first 15 min of data, and average during 15–90 min after inhalation, respectively. Difference between deposition with and without spacer is expressed as effect caused by use of spacer: ([spacer] − [no spacer])/[no spacer]. Positive differences represent increased deposition of drug caused by spacer. Values are expressed as micrograms of TAA deposited in each region. Difference caused by use of spacer (average of all volunteers) is also shown, expressed as percentage of no-spacer value, with negative numbers indicating decrease caused by spacer. This comparison in units of drug mass implicitly uses total dose dispensed from canister as reference quantity.

TABLE 2
Amount of TAA Deposited as Percentage of Inhaled Dose

Region	Spacer (%)	No spacer (%)	Difference	Ratio	% change	*P*
Outer lung	4.98	2.34	2.64	2.1	113	0.0130
Mid lung	2.83	1.17	1.66	2.4	142	0.0028
Bronchial tree	5.76	1.33	4.43	4.3	333	0.0014
Target tissues	13.57	4.85	8.72	2.8	180	0.0027
Lung + airway	17.02	6.76	10.26	2.5	152	0.0029
Mouth	44.91	57.69	−12.78	0.8	−22	0.0763
Mouth (DDV)	37.90	64.20	−26.31	0.6	−41	0.0271

DDV = dose delivered at valve.
Data represent average percentage of inhaled drug deposited in each region in all volunteers during 0–15 min after inhalation. Mouth (DDV) values represent oral deposition as it is commonly reported in inhalation drug literature: sum of mouth, esophagus, stomach, and abdomen regions expressed as percentage of DDV as opposed to inhaled dose.

was analyzed as a percentage of the dispensed dose, the reduction in mouth deposition caused by the spacer was statistically significant ($P = 0.027$).

The regional kinetics of TAA are shown in Figures 5 and 6. Figure 5 shows the contrast between the target regions (from bronchi to outer lung), the entire airway, and the nontarget regions of the mouth and abdomen. Figure 6 shows the breakdown of deposition among the target regions. The data in the figures are percentage of inhaled dose, as in Table 2. However, Table 2 shows averages of the first 15 min after inhalation, and the figures show the individual time-point data. Although the tabular values are less affected by noise and give a better statistical analysis, the initial data points in the plots are more representative of the initial deposition of drug in each region. The difference in deposition caused by the spacer is apparent in both plots, as is absorption and clearance of the drug. Concentration increased only in the gastrointestinal regions, because of a lack of direct deposition there and because of continual swallowing of drug originally deposited in the mouth and airway. As might be expected, Figure 6 shows that airway deposition was highest in the bronchial region, even though the region was small. Deposition in the trachea was greater because of impaction at the bronchial bifurcations, which were clearly seen in the PET images. The concentration of deposited drug continued to decrease distally (Fig. 4), although the larger size of the outer lung region led to higher deposition there. Figures 5 and 6 also show that clearance is not uniform throughout the airway. Clearance from bronchial regions and the trachea was faster than from the lung regions. This finding is consistent with normal mucociliary clearance from the central airways (*22*,*23*). Figure 4 shows a rendering of the PET images obtained from a representative volunteer, overlaid on the CT scan of the same volunteer. The difference in drug distribution caused by the spacer is again apparent. The images are scaled to show equality of their respective inhaled doses.

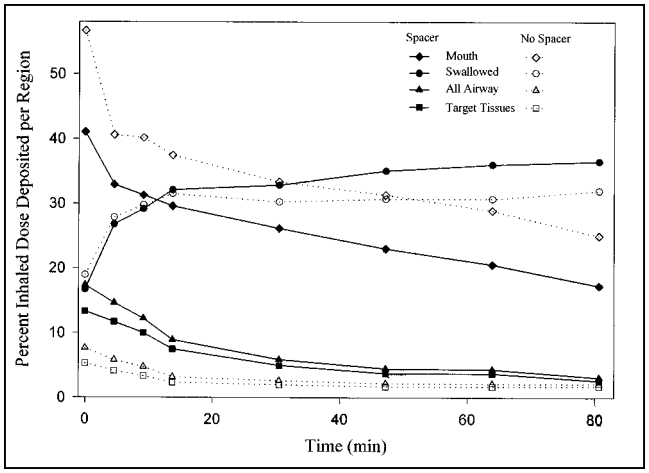

FIGURE 5. Time–dose curves from summary regions. Deposition in high-dose regions combined by function is shown versus time. Data points are placed at beginning of relevant scan period. Swallowed dose (abdomen and esophagus), dose in entire airway (trachea to outer lung), and dose in target tissues (bronchi to outer lung) are shown for deposition with use of spacer and without spacer.

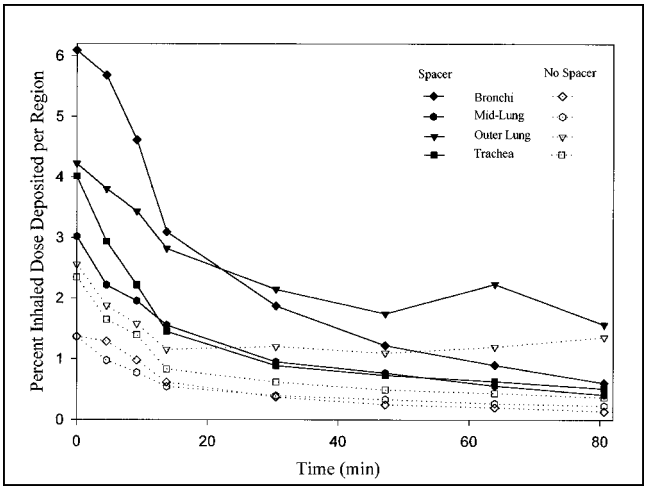

FIGURE 6. Target regions shown as in Figure 5. Deposition in bronchus, mid lung, outer lung, and trachea is shown with use of spacer and without spacer.

DISCUSSION

Several factors are important for measurement of deposited inhaled drug through imaging. Principally, the radiolabeled material must be a valid tracer for the drug of interest, and the imaging and data analysis methods must produce data with an accuracy that justifies the analysis that is being applied. Most commonly, pulmonary aerosol deposition studies have been performed using planar γ imaging with ^{99m}Tc added to the drug formulation as a tracer (*1–7*). Implicit in such studies is the assumption that the only parameter responsible for drug deposition is particle size distribution, which is duplicated as closely as possible when the added tracer is formulated. In practice, the assumption is reasonable, and the initial distribution of tracer probably reflects the initial deposition of inhaled particles. However, planar imaging has well-known limitations for a quantitative pulmonary distribution study. The depth of distribution is not uniform; therefore, attenuation and distance correction is not simple. The attenuation coefficients of tissues in the chest also vary widely. Although a rigorous attempt to correct for variations in scatter, attenuation, and sensitivity may produce a reasonable estimate of relative quantitative distribution (*24*,*25*), a quantitative measurement of dose deposition is not practical. This problem was a motivation in our performing PET measurements. The measured 3-dimensional attenuation correction, scatter correction, and camera calibration in this study are not available to planar imaging. Another strong motivation was the desire to examine changes in drug distribution as a function of time. Such an examination is not possible by adding a nondrug tracer to the formulation; the drug must be labeled and allowed to act as its own tracer. The requirement that the label distribute evenly among the particles in the drug suspension remains important. This requirement was met by determining cascade impactor particle sizes for each dose and by ensuring that the labeled product remained within the manufacturing specifications for the marketed drug.

Acquisition of anatomic images was critically important. The PET images show a few easily identifiable landmarks (bronchial bifurcations, trachea, mouth) but lack the anatomic cues that are commonly seen with intravenous radiopharmaceuticals. Fiducial markers, PET transmission measurements, and emission scans were necessary to aid the alignment of image volumes with CT images. The process resulted in an alignment accurate to within 2 mm and allowed use of the anatomic detail of the CT images for creation of regions of interest that would otherwise be impossible to define reproducibly. Although the alignment was accurate to 2 mm, as measured from fiducial markers and rigid structures, additional alignment challenges are presented by shifts in position, including bending, and respiratory motion. CT images were acquired after the volunteers had been instructed to ventilate well and then assume a resting, rather than fully inflated, inhalation level during breath holding. This tactic was remarkably successful, although it was not perfect. Remaining variations in relative body positions were considered during region-of-interest creation, so that the results for regional activity were accurate for each scan in each dynamic series. Arm and shoulder positioning was similar in each scan to avoid creating internal variations, but the degree of alignment of these tissues in the images was ignored.

The results allow several interesting observations. A striking feature of this study is that the measured TAA initial distribution in the lung is qualitatively very different from all previously reported drug distributions measured by planar imaging. Although some of the previously examined drug formulations were different from this one, studies of similarly formulated metered dose inhalers with drugs of similar particle size are available. In all of those studies, the percentage of central (bronchial and tracheal) deposition of drug was reported to be much less than we have observed, and the percentage of lung deposition was reported to be correspondingly much larger. We believe that this might be explained simply on the basis of the differences between PET scanning and planar imaging. Most of the planar studies did not include attenuation or scatter corrections, and others included only simple global correction factors that do not take into account regional variations. Our confidence in our results arises from calibration measurements made with chest phantoms, from measurement of the doses injected into the fiducial markers, and from previous validated quantitative results obtained with PET (*26–29*).

The tables clearly show the effect of the integrated spacer on deposition in most regions of interest. Because of the greater clinical relevance of distribution as a percentage of the drug dose inhaled, the data in the tables are calculated on that basis. But to best determine the ability of the spacer to decrease oropharyngeal deposition, the commonly reported value is the oral and swallowed dose (sum of mouth, esophagus, stomach, and abdomen) as a percentage of the DDV. On this basis, the spacer was responsible for a 41% decrease in the amount of drug deposited in the mouth. This shows an important function of a spacer device, to decrease total oral corticosteroid deposition and the potential for local side effects.

The TAA initially deposited in the bronchial region and trachea decreased more rapidly than in any other regions, including the mouth. The result was that by 80–90 min after administration, the amount of TAA in the bronchial region, initially twice that in the mid-lung region, had fallen to the same level as in the lung regions. The decrease in labeled TAA from the conducting airways was likely caused by normal mucociliary clearance. Ciliary motion moves foreign particles along the trachea to the pharynx, where they are swallowed. The process can be rapid, with velocities approaching 1 cm/min. By the end of the study, most of the deposited dose that remained in the target regions was found in the outer lung region. In considering these data, one must remember that the regions are of different sizes and that the dose was not uniformly deposited throughout each region. The relative concentration of drug deposited at any particu-

lar lung location, for example, was therefore considerably lower than the concentration deposited on the bronchial tissue, even at the end of the data acquisition. With the integrated spacer, the target tissues initially received 60 μg TAA (Table 1), or 14% of the inhaled dose, and this decreased by a factor of 3 during the time of data acquisition. The amount initially deposited in the outer lung was 9 μg. However, the drug is thought to act by binding at the corticosteroid receptors in the target tissues, where its duration of binding is long (*8,12*). It would be reasonable to expect that low concentrations would be effective or that the absorption rates shown in Figure 6 might be the more relevant parameters to measure if shown to be related to drug that is being dissolved and made available to the tissue. The concentration of drug that needs to be present in tissue to have a therapeutic effect is unknown. Therefore, the data presented here tell us much about the delivery and subsequent presence of the drug on the target tissues. Our results allow an evaluation of the effectiveness of drug delivery to the lungs, as compared with systemic absorption, and an evaluation of the effectiveness of the integrated spacer in modifying drug deposition. But our results cannot tell us what to expect in terms of clinical effectiveness without additional knowledge of the clinical action of the drug. PET studies provide a valuable measurement of the effectiveness of delivery methods and formulations in depositing drug in the target regions and a measurement of the duration of residence of a deposited drug. These are clearly parameters that should be therapeutically important, and knowing their values will allow formulations to be adjusted to perform as desired.

CONCLUSION

The quantitative distribution and kinetics of TAA in the lung, airway, and upper gastrointestinal tract after oral inhalation were successfully measured. In the airway, the heaviest deposition of drug was in the trachea and bronchi, as might be expected, with decreasing deposition in the distal lung. The effect of an inhalation spacer on the dose distribution was striking, with deposition in target regions increased by up to a factor of 4 relative to inhalation without a spacer, and oral deposition reduced by 40% when the spacer was used. The effect of the spacer was shown to be statistically significant with only 5 individuals in the study.

ACKNOWLEDGMENTS

The authors are indebted to Bonnie Landmeier Bennington, Emily Heath Wilson, and Catherine Berridge for technical assistance during the tracer experiments. Medical support from Drs. Jim O'Donnell and Peter Faulhaber is appreciated. Financial support for this study provided by RPR is gratefully acknowledged.

REFERENCES

1. Johnson MA, Newman SP, Bloom R, Talaee N, Clarke SW. Delivery of albuterol and ipratropium bromide from two nebulizer systems in chronic stable asthma: efficacy and pulmonary deposition. *Chest.* 1989;96:6–10.
2. Laube BL, Links JM, Wagner HN Jr, et al. Simplified assessment of fine aerosol distribution in human airways. *J Nucl Med.* 1988;29:1057–1065.
3. Leach CL. Improved delivery of inhaled steroids to the large and small airways. *Respir Med.* 1998;92(suppl A):3–8.
4. Newman SP, Moren F, Pavia D, Little F, Clarke SW. Deposition of pressurized suspension aerosols inhaled through extension devices. *Am Rev Respir Dis.* 1981;124:317–320.
5. Newman SP, Moren F, Trofast E, Talaee N, Clarke SW. Deposition and clinical efficacy of terbutaline sulphate from Turbuhaler, a new multi-dose powder inhaler. *Eur Respir J.* 1989;2:247–252.
6. Newman SP. Scintigraphic assessment of therapeutic aerosols. *Crit Rev Ther Drug Carrier Syst.* 1993;10:65–109.
7. Newman SP, Weisz AW, Talaee N, Clarke SW. Improvement of drug delivery with a breath actuated pressurised aerosol for patients with poor inhaler technique. *Thorax.* 1991;46:712–716.
8. Williams MH Jr. Treatment of asthma with triamcinolone acetonide aerosol. *Chest.* 1975;68:765–768.
9. Kripalani KJ, Cohen AI, Weliky I, Schreiber EC. Metabolism of triamcinolone acetonide-21-phosphate in dogs, monkeys, and rats. *J Pharm Sci.* 1975;64:1351–1359.
10. Mollmann H, Rohdewald P, Schmidt EW, Salomon V, Derendorf H. Pharmacokinetics of triamcinolone acetonide and its phosphate ester. *Eur J Clin Pharmacol.* 1985;29:85–89.
11. O'Byrne PM, Pedersen S. Measuring efficacy and safety of different inhaled corticosteroid preparations. *J Allergy Clin Immunol.* 1998;102:879–886.
12. Smith CL, Kreutner W. In vitro glucocorticoid receptor binding and transcriptional activation by topically active glucocorticoids. *Arzneimittelforschung.* 1998;48:956–960.
13. Bisgaard H, Anhoj J, Klug B, Berg E. A non-electrostatic spacer for aerosol delivery. *Arch Dis Child.* 1995;73:226–230.
14. Goldberg S, Algur N, Levi M, et al. Adrenal suppression among asthmatic children receiving chronic therapy with inhaled corticosteroid with and without spacer device. *Ann Allergy Asthma Immunol.* 1996;76:234–238.
15. Meeran K, Burrin JM, Noonan KA, Price CP, Ind PW. A large volume spacer significantly reduces the effect of inhaled steroids on bone formation. *Postgrad Med J.* 1995;71:156–159.
16. Miller MR, Bright P. Differences in output from corticosteroid inhalers used with a volumatic spacer. *Eur Respir J.* 1995;8:1637–1638.
17. O'Reilly JF, Gould G, Kendrick AH, Laszlo G. Domiciliary comparison of terbutaline treatment by metered dose inhaler with and without conical spacer in severe and moderately severe chronic asthma. *Thorax.* 1986;41:766–770.
18. Zar HJ, Liebenberg M, Weinberg EG, Binns HJ, Mann MD. The efficacy of alternative spacer devices for delivery of aerosol therapy to children with asthma. *Ann Trop Paediatr.* 1998;18:75–79.
19. Berridge MS, Cassidy EH, Bordeaux KG. Preparation of [^{11}C]triamcinolone acetonide. *Appl Radiat Isot.* 1994;45:91–95.
20. Woods RP, Mazziotta JC, Cherry SR. MRI-PET registration with automated algorithm. *J Comput Assist Tomogr.* 1993;17:536–546.
21. Gonzalez RC, Wintz P. *Digital Image Processing.* Reading, MA: Addison-Wesley; 1987:368–375.
22. Wanner A, Salathe M, O'Riordan TG. Mucociliary clearance in the airways. *Am J Respir Crit Care Med.* 1996;154:1868–1902.
23. Mortensen J, Lange P, Nyboe J, Groth S. Lung mucociliary clearance. *Eur J Nucl Med.* 1994;21:953–961.
24. Lee Z, Berridge M, Nelson AD, Heald DL. Evaluation of planar imaging vs. PET for pulmonary deposition of inhaled aerosols: a validation study [abstract]. *J Nucl Med.* 1999;40(suppl):197P
25. Lee Z, Berridge M, Nelson AD, Heald DL. Corrections in gamma scintigraphy [abstract]. *J Aerosol Med.* 1999;12:135.
26. Bednarczyk EM, Green JA, Nelson AD, et al. Comparative assessment of the effect of lomefloxacin, ciprofloxacin, and placebo on cerebral blood flow, and glucose and oxygen metabolism in healthy subjects by positron emission tomography. *Pharmacotherapy.* 1992;12:369–375.
27. Berridge MS, Adler LP, Nelson AD, et al. Measurement of human cerebral blood flow with [^{15}O]butanol and positron emission tomography. *J Cereb Blood Flow Metab.* 1991;11:707–715.
28. Muzic RF Jr, Berridge MS, Zheng L, Nelson AD, Miraldi F. PET measurement of beta-adrenergic receptor concentration using [F-18]fluorocarazolol [abstract]. *J Nucl Med.* 1996;37(suppl):P174.
29. Muzic RF Jr, Berridge MS, Friedland RP, Zhu N, Nelson AD. PET quantification of specific binding of [^{11}C]nicotine in human brain. *J Nucl Med.* 1998;39:2048–2054.

The Journal of NUCLEAR MEDICINE

Pulmonary Distribution and Kinetics of Inhaled [^{11}C]Triamcinolone Acetonide

Marc S. Berridge, Zhenghong Lee and Donald L. Heald

J Nucl Med. 2000;41:1603-1611.

The Journal of Nuclear Medicine is published monthly.
SNMMI | Society of Nuclear Medicine and Molecular Imaging
1850 Samuel Morse Drive, Reston, VA 20190.
(Print ISSN: 0161-5505, Online ISSN: 2159-662X)

SNMMI SOCIETY OF NUCLEAR MEDICINE AND MOLECULAR IMAGING